Journal of Thermal Analysis and Calorimetry, Vol. 62 (2000) 211–225

Al–Ga–Zn PHASE DIAGRAM
Calorimetric study of the isobaric invariants

*E. Aragon, K. Jardet, P. Satre and A. Sebaoun**

Laboratoire de Physico-Chimie du Matériau et du Milieu Marin, Matériaux à Finalité Spécifique (E.A. 1356), Université de Toulon et du Var, B.P. 132, 83957 La Garde Cedex, France

(Received October 18, 1999)

Abstract

The Al–Ga–Zn ternary phase diagram presents two isobaric invariant reactions: a eutectic at 23±1°C and a metatectic at 123±1°C [1–3]. Calorimetric measurements on the two isobaric invariant reactions have been carried out. First the Tammann method has enabled us to determine the composition of their limits on five isopletic cross sections. Then, the compositions of the invariant phases have been determined.

Keywords: calorimetric measurements, phase diagram, Tammann's method, ternary system Al–Ga–Zn

Introduction

In previously published papers [1–2], we have proposed an Al–Ga–Zn phase diagram (Figs 1 and 2). In those papers, the stability fields of the phases in equilibrium as well as the ternary isobaric invariants have been determined. Studies have been carried out by the isopleth cutting method by using coupled direct and differential thermal analysis, X-ray diffraction at various temperatures and electron probe microanalysis. Six isopletic cross sections had been established. On these isopletic cross sections, two isobaric invariant reactions had been observed:

– A ternary eutectic: $Ga_{SS} + Zn_{SS} + \alpha_{SS} \Leftrightarrow L_E$ $\Delta H_E > 0$

– A ternary metatectic: $Zn_{SS} + \alpha_{SS} + L_M \Leftrightarrow \alpha'_{SS}$ $\Delta H_M > 0$

The temperatures of these two ternary invariant reactions (23±1°C and 123±1°C, respectively) have been determined on heating by calorimetric measurements.

* Author for correspondence: Phone: 33-4-94-14-23-05; fax: 33-4-94-14-23-42; E-mail: sebaoun@univ-tln.fr

1418–2874/2000/ $ 5.00

Akadémiai Kiadó, Budapest
Kluwer Academic Publishers, Dordrecht

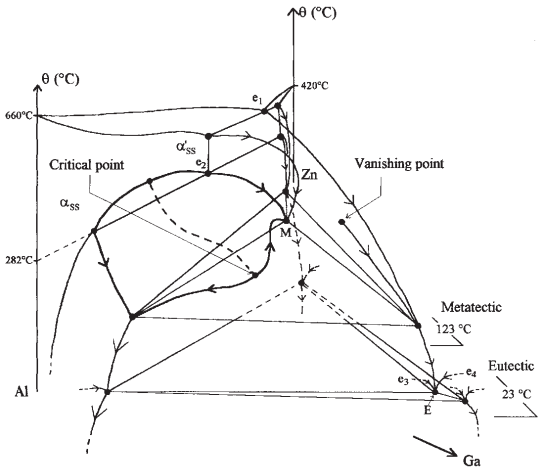

Fig. 1 Al–Ga–Zn diagram: monovariant lines and ternary invariant reactions

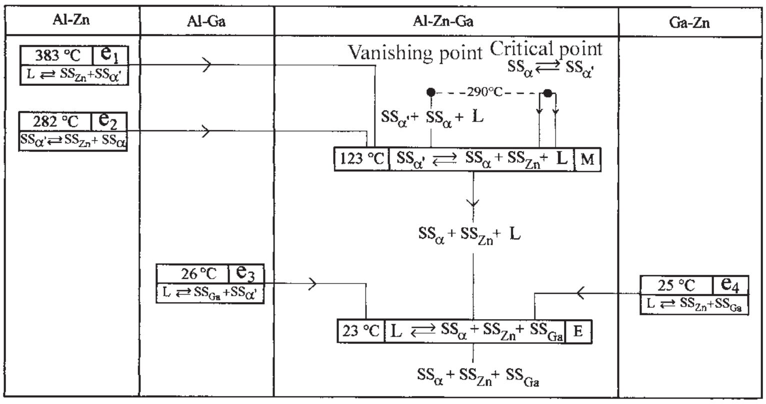

Fig. 2 Al–Ga–Zn diagram: reaction scheme

First, they enabled us to determine the limits of the invariant triangles on each isopletic cross section and then, to determine that triangles at the two invariant temperatures.

Theoretical approach: the Tammann method

A well-known method for determining the composition of the binary invariant point has been established by Tammann at the beginning of the century [4–6]. This method has been widely used on the binary invariant reactions but concerning its application to ternary phase diagrams only few bibliographic data are available. The method has been described for few particular and theoretical cases of ternary systems [7]. However, rare works have been experimentally performed on that topic. In 1911, Loebe

[8] has presented twelve isopletic cross sections in the Pb_6Sb–Sn ternary system and the evolutions of the enthalpies associated with the invariant reactions have been followed on these sections. Tammann *et al.* [9] in 1925 have applied the method to the quasi-binary section Pb–Zn_3Sb_2 in the Pb–Sb–Zn ternary system for determining the composition of the eutectic point on this section. In 1984, Tenu and Counioux [10] proposed a quantitative method which consists in measuring the enthalpies associated with the ternary invariant reaction for several compositions and to deduce from these measurements the composition of the eutectic point using the less square method. The precision of these method depends on the experimental parameters, particularly the heating rate.

Legendre *et al.* [11] have applied that qualitative method to the ternary system Au–Sb–Si. A similar method, applied to binary alloys of energetic materials, has been developed by Zi–Ru Liu *et al.* [12] and extended to ternary alloys [13] in order to determine the eutectic composition.

The Tammann's diagrams are based on the proportional variation of the heat quantity as a function of the mass of the phase formed or decomposed during the invariant reaction. That evolution is linear if all the calorimetric values measured on samples having an identical mass, are given in the correct unit (J g^{-1}) [for a representation in atomic% the heat of reaction would be in this case given in J mol^{-1}], moreover, if the composition scale is represented in mass percent** [14]. These general remarks are true in binary as well as in ternary phase diagrams on isopletic cross sections. As a consequence, for an invariant reaction (Fig. 3):

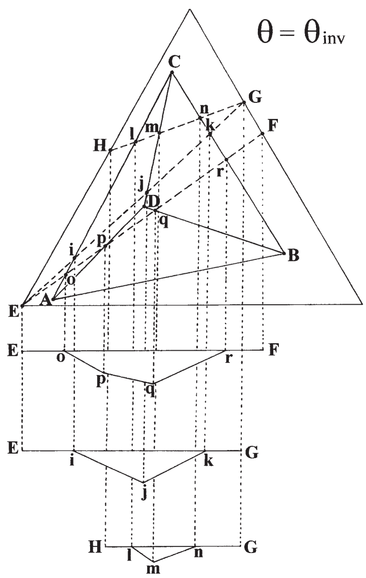

Fig. 3 Enthalpies evolution on isopletic cross sections in a ternary phase diagram

** The composition will always be given in mass percent.

$$A + B + C \Leftrightarrow D \qquad \Delta H_{Inv} > 0$$

a linear evolution is observed on the particular EF isopletic cross section (Fig. 3) as, in the general case, on the GH isopletic cross section (Fig. 3).

Experimental

The samples were prepared by weighing and melting pure Al, Zn and Ga (99.999%) in cast iron crucibles with an internal graphite coating under nitrogen atmosphere.

This experimental study has been carried out by using the isopletic cross sections method. Four main isopletic cross sections (Fig. 4) have been chosen: ZA7–Ga ($m_{Al}/(m_{Al}+m_{Zn})=0.07$) , ZA15–Ga, ZA20–Ga and ZA40–Ga. In addition, two isopletic cross sections have been partly studied in order to determine the limits of the isobaric ternary invariants in the Al-rich corner: ZA74–AGa52 and ZA88–AGa22 (Fig. 4).

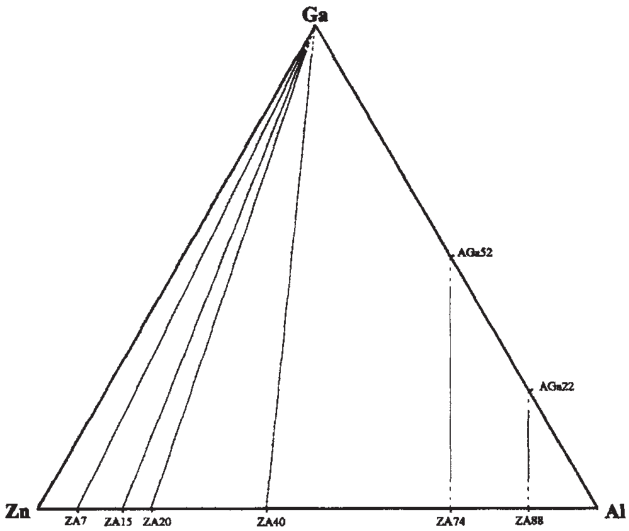

Fig. 4 Al–Zn–Ga diagram: isopletic cross sections for the experimental study

A differential scanning calorimeter (DSC 92 – Setaram) has been used: it allows invariant calorimetric measurements and low temperatures investigations by cooling in liquid nitrogen. Crucibles in stainless steel sealed with copper joins were used to prevent zinc vaporization and alloys oxidation. The used temperature range was from –50 to 550°C. The thermal analysis curves have been recorded both on heating and cooling. A heating and cooling rate of 5°C min^{-1} has been chosen. The enthalpic measurements have been carried out on heating. The accuracy of the enthalpic measurements obtained after calibration is about 10% for composition determination and ±1°C for temperature one. Each composition on the different isopletic cross sections has been studied by three successive thermal cycles.

The method used for determining the compositions of the invariant phases is based on an interpolative and iterative process. The main limit condition (ΔH_{Inv}=0) is verified on the limits of the invariant reaction. On the other hand, the ΔH_{Inv} value is maximal at the invariant point (eutectic liquid L_E or α'_{SS} metatectic phase). For any composition concerned by the invariant reaction, the ΔH_{Inv} value is proportional to the quantity of the invariant phase formed on heating. This quantity is given by a barycentric relation at the end of the invariant reaction which corresponds to an indifferent equilibrium.

Results

Temperatures of the stable and metastable invariant equilibria

The two isobaric invariant reactions have been identified on heating at 23±1°C for the ternary eutectic and at 123±1°C for the ternary metatectic.

Table 1 Al–Ga–Zn diagram: invariant temperatures (heating and cooling) and enthalpies (on heating) as a function of alloys composition on the ZA74–AGa52 isopletic cross section

Mass percent of gallium on the isopletic cross section ZA74–AGa52			10	15	20	25	30	35	40	45
Metatectic	θ_{inv}/°C	heating			123	122	123			
		cooling			103	102	103			
	Enthalpies/J g^{-1}				1.8	1.2	0.5			
Eutectic	θ_{inv}/°C	heating		23	23	22	23	24	23	23
	Enthalpies/J g^{-1}			3.1	6.8	10.2	14.8	16.4	22	25.7

Table 2 Al–Ga–Zn diagram: invariant temperature(s) and enthalpies (on heating) as a function of alloys composition on the ZA88–AGa22 isopletic cross section

Mass percent of gallium on the isopletic cross section ZA88–AGa22			5	10	15	20
Metatectic	θ_{inv}/°C	heating				
		cooling				
	Enthalpies/J g^{-1}					
Eutectic	θ_{inv}/°C	heating			23	
	Enthalpies/J g^{-1}				0.5	

On cooling the boundaries of the three-phase region (Zn_{SS}+α_{SS}+α'_{SS}) and the eutectic transformation are displaced towards lower temperatures. The metatectic reaction is measured at 102±1°C (Tables 1 to 6 and Fig. 5). The eutectic transformation is displaced from 23°C on heating to –3°C on cooling. But thermal accidents are observed up to –30°C on cooling depending on sample compositions (Table 4 and

Table 3 Al–Ga–Zn diagram: invariant temperatures (heating and cooling) and enthalpies (on heating) as a function of alloys composition on the ZA7–Ga isopletic cross section

Mass percent of gallium on the isopletic cross section ZA7–Ga			0	2	5	7.5	10	13.5	15	17.5	20	22.5
Metatectic	θ_{inv}/°C	heating			123	123	123	124	123	124	122	124
		cooling			101	102	102	103	102	102	103	102
	Enthalpies/J g^{-1}				1.1	3.0	5.0	5.6	5.6	6.0	5.2	4.7
Eutectic	θ_{inv}/°C	heating			23		23					
	Enthalpies/J g^{-1}				1.9		4.5					

Mass percent of gallium on the isopletic cross section ZA7–Ga			25	28	31	35	41	45	54	63	77	93
Metatectic	θ_{inv}/°C	heating	123	124	124	122	123	123	123	123		
		cooling	101	101	102	102	102	102	103	102		
	Enthalpies/J g^{-1}		4.8	4.7	4.3	4.0	3.6	2.5	2.2	1.3		
Eutectic	θ_{inv}/°C	heating	23					23				
	Enthalpies/J g^{-1}		17					33				

Table 4 Al–Ga–Zn diagram: invariant temperatures (heating and cooling) and enthalpies (on heating) as a function of alloys composition on the ZA15–Ga isopletic cross section

Mass percent of gallium on the isopletic cross section ZA15–Ga			0	2.5	5	10	14.1	17.5	20	25	27.5
Metatectic	θ_{inv}/°C	heating			123	123	122	123	124	124	122
		cooling			102	102	101	102	102	102	102
	Enthalpies/J g^{-1}				0.1	4.3	7.7	9.5	9.5	8.2	8.0
Eutectic	θ_{inv}/°C	heating			23	22	22	24	23	23	23
		cooling			–3	–3	–3	–3	–2	–2	–3
						–17	–5	–19	–3	–14	–12
	Enthalpies/J g^{-1}				1.7	3.3	6.8	9.4	13	17	23

Mass percent of gallium on the isopletic cross section ZA15–Ga			30	40	50	55	60	70	80	90	95
Metatectic	θ_{inv}/°C	heating	123	123	124	122	123	123			
		cooling	101	102	102	102	102	103			
	Enthalpies/J g^{-1}		10.4	8.1	5.8	4.8	3.9	2.0			
Eutectic	θ_{inv}/°C	heating	24	22	23	23	24	23	24	23	23
		cooling	–2	–3	–4	–3	–4	–4	–4	–3	–2
			–10	–9	–21	–12	–19	–17	–30	–24	–21
	Enthalpies/J g^{-1}		24	30	39	44	51	57	67	78	82

Table 5 Al–Ga–Zn diagram: invariant temperatures (heating and cooling) and enthalpies (on heating) as a function of alloys composition on the ZA20–Ga isopletic cross section

Mass percent of gallium on the isopletic cross section ZA20–Ga			0	5.3	11	17	21	25.5	27.3	32
Metatectic	θ_{inv}/°C	heating			122		123	124	122	123
		cooling			102	102	102	103	102	101
	Enthalpies/J g^{-1}				3.0	7.0	9.1	9.5	10.3	8.5
Eutectic	θ_{inv}/°C	heating			23	22		24		
	Enthalpies/J g^{-1}				3.4	8.1		15		

Mass percent of gallium on the isopletic cross section ZA20–Ga			41	51	59	67	75	82	90	95.5
Metatectic	θ_{inv}/°C	heating	123	123	124	122	123			
		cooling	102	102	102	103	103			
	Enthalpies/J g^{-1}		7.2	5.1	4.0	1.9	0.5			
Eutectic	θ_{inv}/°C	heating	23	24						
	Enthalpies/J g^{-1}		26	34						

Table 6 Al–Ga–Zn diagram: invariant temperatures (heating and cooling) and enthalpies (on heating) as a function of alloys composition on the ZA20–Ga isopletic cross section

Mass percent of gallium on the isopletic cross section ZA40–Ga			0	5	10	12	15	20	22	23	25
Metatectic	θ_{inv}/°C	heating				123	122	123	122	122	122
		cooling				103	103	102	101	101	101
	Enthalpies/J g^{-1}					1.3	2.3	4.0	5.2	5.1	5.1
Mass percent of gallium on the isopletic cross section ZA40–Ga			27	30	35	37.5	40	42.5	50	60	70
Metatectic	θ_{inv}/°C	heating	122	123	123	122	121	123	123	122	123
		cooling	102	101	101	102	101	102	102	103	101
	Enthalpies/J g^{-1}		5.3	5.0	4.3	4.1	4.0	3.9	2.7	1.28	0.4

Fig. 5b). These accidents seem to correspond to the crystallization of two allotropic forms of gallium which are metastable at the atmospheric pressure [15–17]. As a consequence, a liquid phase appears at 23°C on heating and can stay present on cooling up to –30°C for some alloys.

Enthalpic measurements on the isopletic cross sections

Enthalpic measurements have been carried out on the four main isopletic cross sections and for the two invariant reactions (Tables 1 to 6).

The metatectic reaction has been studied in order to determine the composition of the invariant phases. For that, the limits of the metatectic invariant (compositions

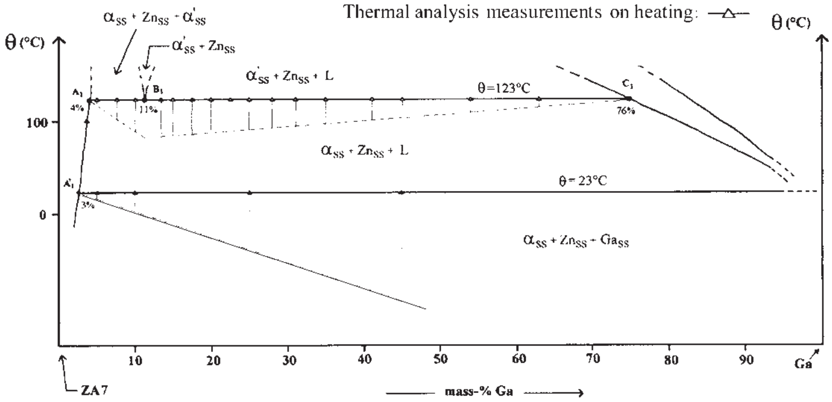

Fig. 5a Al–Ga–Zn diagram: ZA7–Ga isopletic cross section

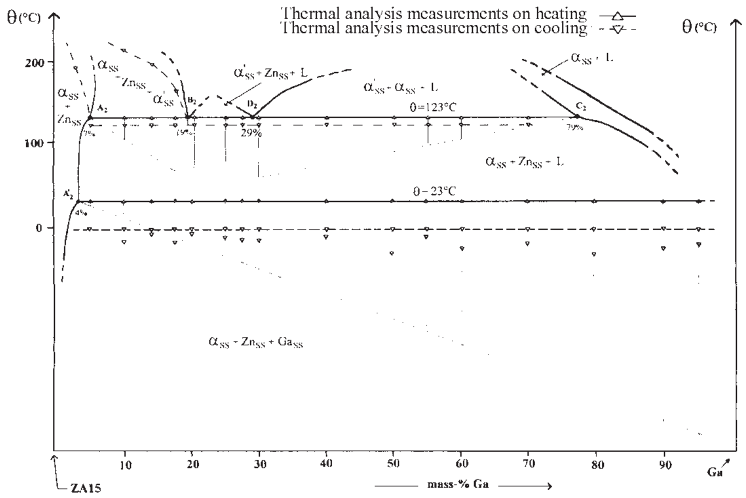

Fig. 5b Al–Ga–Zn diagram: ZA15–Ga isopletic cross section

of the A_i and C_i points: Fig. 5) have been previously determined on each cross section by using the Tammann method. The compositions of the points B_i have also been de-

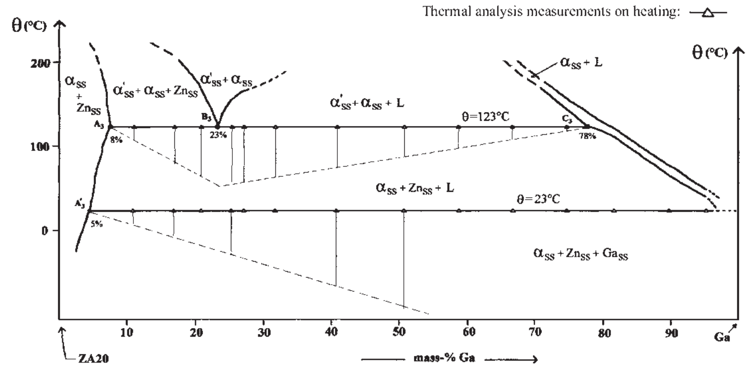

Fig. 5c Al–Ga–Zn diagram: ZA20–Ga isopletic cross section

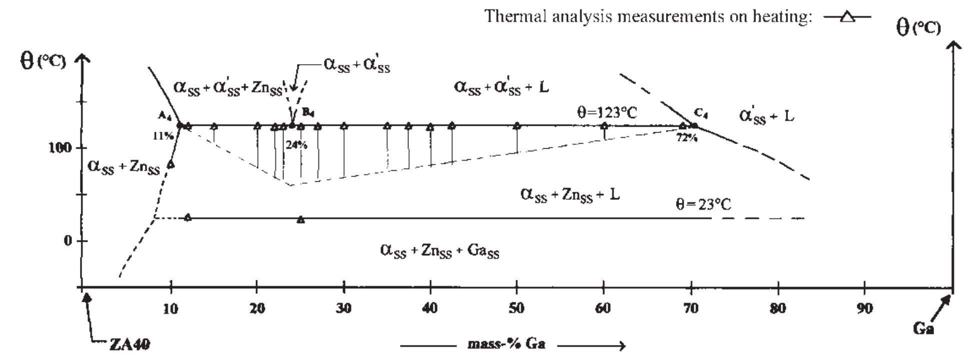

Fig. 5d Al–Ga–Zn diagram: ZA40–Ga isopletic cross section

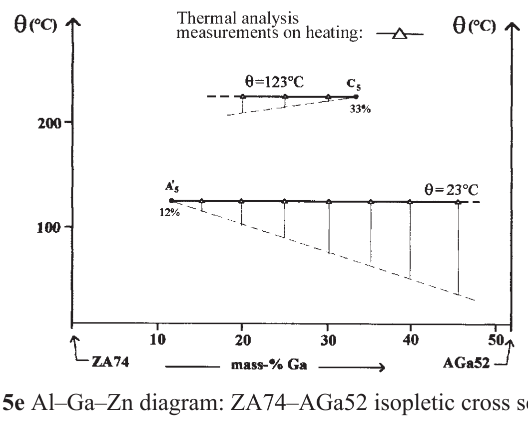

Fig. 5e Al–Ga–Zn diagram: ZA74–AGa52 isopletic cross section

termined (Fig. 5). The accuracy for the determination of C_i is better than the determination of A_i because of a larger composition gap between B_i and C_i than between A_i and B_i. The determination of the points A_5 and B_5 on the ZA74–AGa52 isopletic cross section have not been possible for this reason. On the ZA15–Ga isopletic cross section (Fig. 5-b), between 19 and about 29% of gallium, the enthalpic values are similar and do not show a linear change.

This behaviour is due to the nearness of the metatectic point (Fig. 6a) which is confirmed by the highest enthalpic values measured for these compositions. In fact, two different maxima (B_2 and D_2) are observed on that cross section. The composition of B_2 can be determined with a correct accuracy: it corresponds to the composition for which the enthalpic values become almost constant (between 17.5 and 20%: Table 4). Using the same reasoning, the composition of D_2 seems to be below 30%. But Fig. 6a shows that the ZA15–Ga isopleth is nearly parallel to the ($M–L_M$) tie-line on which D_2 is located. The composition of D_2 is therefore very difficult to determine. The compositions of the A_i, B_i and C_i points are given in Table 7.

Table 7 Compositions (mass% Ga) of the limits of the metatectic reaction on the studied isopletic cross sections

ZA7–Ga		ZA15–Ga		ZA20–Ga		ZA40–Ga		ZA74–AGa52	
A_1	4	A_2	7	A_3	8	A_4	11	A_5	–
B_1	11	B_2 D_2	19 ≈29	B_3	23	B_4	24	B_5	–
C_1	76	C_2	79	C_3	78	C_4	72	C_5	33

On the other hand, the limits of the eutectic reaction have also been studied. Because of the composition of the eutectic point (about 95% [18]), a linear change of the enthalpic values is observed on a large field of compositions. Our measurements do not allow to precise the equilibria in the Ga-rich corner. Then, the A'_i points have only been determined but with a good accuracy because the isopletic cross sections intersect perpendicular to the iso-enthalpic lines (Fig. 5). Their compositions are given in Table 8:

Table 8 Compositions (mass% Ga) of the limits of the eutectic reaction on the studied isopletic cross sections

ZA7–Ga		ZA15–Ga		ZA20–Ga		ZA74–AGa52	
A'_1	3	A'_2	4	A'_3	5	A'_5	12

Determination of the composition of phases for the invariant reactions

Using the A_i, B_i and C_i positions, the compositions of the metatectic invariant phases have been determined. The determination of the composition of the α_{ss} metatectic phase is the more accurate: it corresponds to the intersection point between the three ($A_1–A_2–A_3–A_4–A_5$), ($B_3–B_4$) and ($C_2–C_3–C_4–C_5$) straight lines. The compositions of the other phases participating to the metatectic reaction are determined identically.

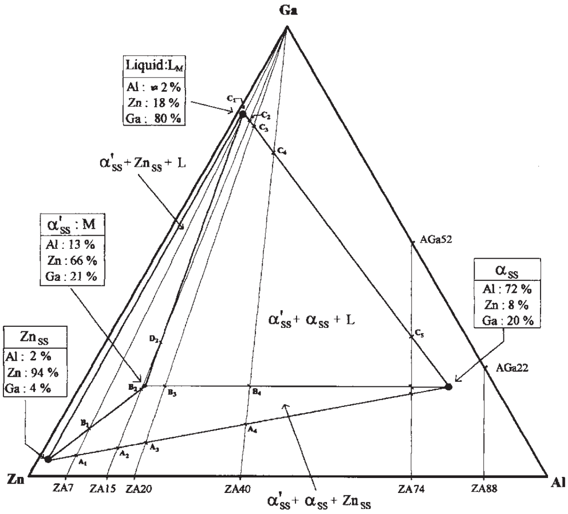

Fig. 6a Al–Ga–Zn diagram: isobaric eutectic at 23°C

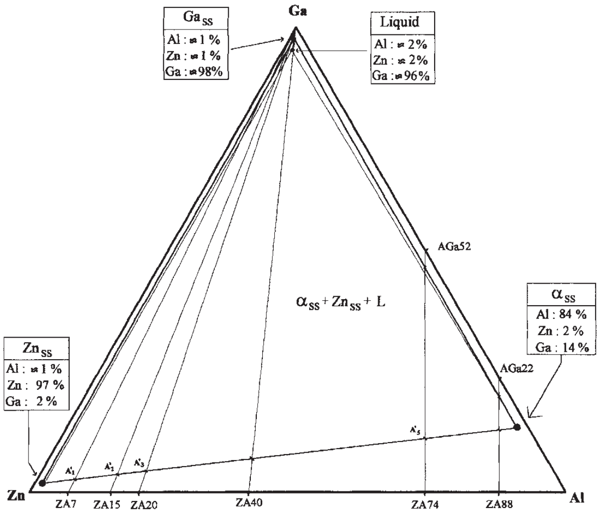

Fig. 6b Al–Ga–Zn diagram: isobaric eutectic at 123°C

Less information is available for determining the eutectic invariant phases. The α_{ss} eutectic phase is located on the (A'_1–A'_2–A'_3–A'_5) well defined straight line which allows to determine its gallium composition. The enthalpic measurement obtained on the ZA88–AGa22 isopletic cross section (Table 2) allowed to conclude that its zinc composition is lower than 5% and a more in-depth analysis of the enthalpic data obtained on the ZA74–AGa52 isopletic cross section (Table 2 and Fig. 5e) conducts to the composition given in Table 9. The composition of Zn_{ss} phase for the metatectic reaction is also determined with a low uncertainty. Some thermal analysis experiments conducted in the Ga-rich corner have allowed us to confirm the compositions of the eutectic Ga_{ss} and liquid phases given by Ansara [18].

The composition of the invariant phases determined by the Tammann method are summarized in Table 9.

The gallium solubility in the α_{ss} ternary solid solution at 23°C (about 14% – Fig. 6a) is lower than those in the α_{ss} binary solid solution (about 20%) given at 26°C [19]. Moreover, that miscibility evolves from 14% at 23°C to 20% at 123°C (Fig. 6b) in the ternary diagram. On the other hand, the miscibility of zinc seems to be approximately constant and at a low value (about 5%).

Table 9 Al–Ga–Zn diagram: isobaric invariant equilibria – composition of the invariant phases

Type	Phases	Composition/mass%±2%		
		Al	Zn	Ga
Metatectic	L_M	≈2	18	80
	α_{SS}	72	8	20
	α'_{SS}	13	66	21
	Zn_{SS}	2	94	4
Eutectic	L_E	≈3	≈3	≈94
	α_{SS}	84	2	14
	Zn_{SS}	≈1	97	2
	Ga_{SS}	≈2	≈2	≈96

Conclusions

This study allowed to confirm the composition of invariant phases and temperature for the eutectic-type isobaric invariant obtained by modelling from the three binary of the bibliography.

Concerning the metatectic isobaric invariant observed at 123°C, it does not agree with the first class peritectic one proposed by bibliography at 282°C [18]. We have determined the composition of the invariant phases.

* * *

The authors thank the D.G.A./D.C.N. (Délégation Générale de l'Armement/Direction des Constructions Navales) of Toulon for financial support during the thesis preparation of E. Aragon at Toulon University. In particular, the help of Mr. Giroud is gratefully acknowledged.

References

1 E. Aragon, K. Jardet, P. Satre and A. Sebaoun, Al–Zn–Ga phase diagram: Part I, J. Therm. Anal. Cal., 53 (1998) 769.
2 E. Aragon, K. Jardet, P. Satre and A. Sebaoun, Al–Zn–Ga phase diagram: Part II, J. Therm. Anal. Cal., 53 (1998) 785.

3 E. Aragon, Thesis, Toulon University, France (1995).
4 G. Tammann, Z. Phys. Chem., 37 (1903) 303.
5 G. Tammann, Z. Phys. Chem., 45 (1905) 24.
6 G. Tammann, Z. Phys. Chem., 47 (1905) 289.
7 M. Sahmen and A. V. Vegesack, Z. Phys. Chem., 59 (1907) 257.
8 V. R. Loebe, Metallurgie, 8 (1911) 7.
9 G. Tammann and O. Dahl, Z. Anorg. U. All. Chem., 144 (1925) 1.
10 R. Tenu and J. J. Counioux, Communication aux J.E.E.P., Tours (1984).
11 B. Legendre and Chay Hancheng, Bull. Soc. Chim. Fr., 2 (1986) 138.
12 Zi-Ru Liu, Ying-Hui Shao, Cui-mei Yin and Yang-Hui Kong, Thermochim. Acta, 250 (1995) 65.
13 Cui-mei Yin, Zi-Ru Liu, Ying-Hui Shao and Yang-Hui Kong, Thermochim. Acta, 250 (1995) 77.
14 A. P. Rollet and R. Bouaziz, L'Analyse Thermique (tome 1), Gauthier Villars ed., Paris 1972.
15 A. Defrain, I. Epelboin and M. Erny, C.R.A.S., 250 (1960) 2553.
16 A. Defrain and I. Epelboin, C.R.A.S., 249 (1959) 50.
17 P. W. Bridgman, Phys. Rev., 48 (1935) 893.
18 I. Ansara, G. Petzow and G. Effenberg ed., Ternary Alloys, 5 (1991) 552.
19 T. B. Massalski, Binary Alloy Phase Diagrams (2nd Edition), B. Massalski ed., 1992.